Cancer Chemother Pharmacol (2000) 46: 416–422

ORIGINAL ARTICLE

**Chun Li · Robert A. Newman · Qing-Ping Wu
Shi Ke · Wei Chen · Toni Hutto · Zuxing Kan
Melvin D. Brannan · Chusilp Charnsangavej
Sidney Wallace**

Biodistribution of paclitaxel and poly(L-glutamic acid)-paclitaxel conjugate in mice with ovarian OCa-1 tumor

Received: 22 December 1999 / Accepted: 24 May 2000

Abstract *Purpose*: Poly(L-glutamic acid)-paclitaxel (PG-TXL) is a water-soluble paclitaxel (TXL) conjugate made by conjugating TXL to poly(L-glutamic acid) via ester bonds. In preclinical studies, PG-TXL has shown significant antitumor activity against a variety of solid tumors. To elucidate the relationship between tissue distribution and antitumor efficacy of PG-TXL, we studied and compared the biodistribution of PG-TXL and TXL. *Methods*: Female C3Hf/Kam mice bearing syngeneic ovarian OCa-1 tumors were injected with either [^{3}H]TXL or PG-[^{3}H]TXL at an equivalent TXL dose of 20 mg/kg. Mice were killed at various times after drug injection, and samples of blood, spleen, liver, kidney, lung, heart, muscle, brain, fat, and tumor were removed and the radioactivity counted. In addition, concentrations of free [^{3}H]TXL released from PG-[^{3}H]TXL in the spleen, liver, kidney, and tumor were analyzed by using high-performance liquid chromatography (HPLC). Whole-body autoradiographs of mice killed 1 day and 6 days after administration of PG-[^{3}H]TXL were obtained to study the intratumoral distribution of PG-TXL. *Results*: When [^{3}H]TXL was conjugated to polymer, the biodistribution pattern of PG-[^{3}H]TXL differed from that of [^{3}H]TXL. Based on area under the tissue concentration-time curve (AUC) values, tumor exposure to [^{3}H]TXL was five times greater when administered as PG-TXL than as TXL formulated in Cremophor EL/alcohol vehicle. Furthermore, concentrations of free paclitaxel released from PG-[^{3}H]TXL remained relatively constant in tumor tissue, being 489, 949 and 552 ng/g tumor tissue at 5, 48 and 144 h after dosing, respectively. Autoradiographic images of mice injected with PG-[^{3}H]TXL revealed that radioactivity was primarily located in the periphery of the tumor on day 1 after drug administration and was homogeneously diffused into the center of the tumor by day 6. Over the 144-h study period, [^{3}H]TXL concentrations, predominantly as the inactive conjugate, were higher in tissues with a more abundant reticular endothelial system (i.e. liver, kidney, spleen, lung) than in tissues with less abundant or lacking RE systems (i.e. muscle, fat, brain). Both [^{3}H]TXL and PG-[^{3}H]TXL were excreted primarily through the hepatobiliary route, with a small fraction of each drug (5% and 8.7%, respectively) excreted into the urine within 48 h. *Conclusions*: This study indicates that the distribution to tumor tissue was enhanced when [^{3}H]TXL was administered as a macromolecular conjugate, and that free TXL was released and maintained within the tumor for a prolonged period. Thus, the antitumor activity of PG-TXL observed in preclinical studies may be attributed in part to enhanced tumor uptake of PG-TXL.

Key words Paclitaxel · Poly(L-glutamic acid) · Polymeric drugs · Biodistribution

This work was supported in part by grants R29-CA74819 and R41-CA80589 from the National Institutes of Health, by the John S. Dunn Foundation and the Gianturco Fund, and by a grant from Cell Therapeutics, Inc.

C. Li (✉) · Q.-P. Wu · S. Ke · Z. Kan
C. Charnsangavej · S. Wallace
Department of Diagnostic Radiology,
The University of Texas M. D. Anderson Cancer Center,
1515 Holcombe Boulevard, Houston, Texas 77030, USA
e-mail: cli@di.mdacc.tmc.edu
Tel.: +1-713-7925182; Fax: +1-713-7945456

R. A. Newman · W. Chen · T. Hutto
Department of Clinical Investigation,
The University of Texas M. D. Anderson Cancer Center,
Houston, Texas, USA

M. D. Brannan
Cell Therapeutics, Inc., Seattle,
Washington, USA

Introduction

Paclitaxel (Taxol, TXL) has shown significant antitumor activity in patients with ovarian, breast, head and neck cancer, and non-small-cell lung carcinomas as well as

sarcomas [8, 18]. The use of TXL is, however, limited by the drug's toxicity (i.e. acute myelosuppression and peripheral neurotoxicity) and limited aqueous solubility. The toxicity of TXL is related to the time that the drug exceeds plasma threshold levels in the range 50–100 n*M* (43–85 ng/ml) [21]. Because TXL has limited solubility in water, it is currently formulated as a concentrated solution containing 6 mg TXL/ml Cremophor EL and ethyl alcohol (50% v/v) that must be further diluted before administration [7]. Several toxic effects have been attributed to Cremophor EL, including serious hypersensitivity reactions [4, 23]. Current clinical protocols call for infusion of TXL over 3–24 h and premedication with corticosteroids and antihistamines [8]. Numerous attempts have been made to develop TXL formulations with reduced systemic toxicity and an enhanced therapeutic index by using water or other vehicles that are safer and better tolerated than Cremophor EL. These attempts have included the use of liposomes [20], microspheres [1], micelles [24], prodrugs [15, 17], and polymer-drug conjugates [9, 11].

We have previously shown that TXL becomes highly water soluble when it is covalently conjugated to poly(L-glutamic acid) (PG). More importantly, the resulting conjugate, PG-TXL, is less toxic than TXL and shows significant antitumor activity against various murine and human tumors [11, 12]. The pharmacokinetics of PG-TXL in mice are notable: PG-TXL has a much longer plasma residence time than TXL, and only a small amount of free TXL is present in the plasma after i.v. injection of PG-TXL [11].

The biodistribution of TXL in rodents has been described before. When administered as free drug, TXL is distributed extensively into normal tissues except for the brain and testes [2, 6, 10, 21]. Distribution studies in tumor-bearing mice have shown high TXL concentrations in the liver and tumor at 24 h after administration [2]. Similar distribution behavior has been also observed with indium-111-labeled TXL [10]. In the present study, the biodistributions of [^{3}H]TXL and PG-[^{3}H]TXL administered intravenously to C3Hf/Kam mice with murine ovarian OCa-1 tumor were determined and compared. In addition, concentrations of free [^{3}H]TXL in various tissues after PG-[^{3}H]TXL injection were analyzed using high-performance liquid chromatography (HPLC) to characterize the in vivo release of [^{3}H]TXL from PG-[^{3}H]TXL.

Materials and methods

Drugs

TXL was obtained from Hande Technology (Houston, Tx.). [^{3}H]TXL (specific activity 19.2 mCi/mg) was obtained from Moravek Biochemicals (Brea, Calif.). This preparation contained a mixture of [^{3}H]TXL species with the majority of the tritium distributed in the aromatic rings. To prepare the injection solution, unlabeled TXL was dissolved in methanol and mixed with the stock solution of [^{3}H]TXL to give [^{3}H]TXL with a specific activity of 17.3 μCi/mg (38,421 dpm/μg). After evaporation of methanol, [^{3}H]TXL was redissolved in Cremophor/alcohol (1:1, v/v) at a concentration of 10 mg/ml and this solution was further diluted with sterile saline (1:4, v/v) such that an i.v. bolus TXL dose of 20 mg/kg could be delivered in a volume of 0.3 ml.

PG, molecular weight 31–39 kDa, was obtained from Sigma Chemical Co. (St. Louis, Mo.). PG-[^{3}H]TXL conjugate was synthesized from PG and [^{3}H]TXL using a previously described procedure [11]. The resulting conjugate contained 20% (w/w) TXL, and the specific activity was 2.30 μCi/mg conjugate or 11.5 μCi/mg equivalent TXL (25,535 dpm/μg). Before injection, the conjugate was dissolved in saline to an equivalent TXL concentration of 4 mg/ml and filtered through a 0.22-μm sterile filter.

Both [^{3}H]TXL and PG-[^{3}H]TXL were delivered at an equivalent TXL dose of 20 mg/kg body weight.

Animals

Female C3Hf/Kam mice (25–30 g) were bred and maintained in a specific pathogen-free mouse colony in the Department of Experimental Radiation Oncology. All experiments involving animals were performed in accordance with the guidelines of the institution's Animal Care and Use Committee. Solid tumors were produced in the mice by injecting 5×10^5 murine ovarian carcinoma OCa-1 cells into the muscle of the right thigh. When the average of three orthogonal tumor diameters reached 6–8 mm, radiolabeled drugs were injected into the tail vein.

Tissue sample collection, counting of radioactivity, and biodistribution

At 2, 5, 24, 48, and 144 h after injection of either [^{3}H]TXL or PG-[^{3}H]TXL, animals were killed, and 0.3 ml whole blood was collected into a tube containing 10 U heparin. Various tissue samples were removed, weighed, dissected, and homogenized with three volumes (w/v) of phosphate-buffered saline (PBS). Aliquots of tissue homogenate were mixed with tissue solubilizer (Packard, Meriden, Ct.). Scintillation solvent was added, and the total radioactivity in the mixtures was counted. The counting efficiency was verified by the method of standard addition. The concentrations of equivalent [^{3}H]TXL in each sample were calculated using the known specific activity of the administered [^{3}H]TXL and PG-[^{3}H]TXL and are expressed as nanograms per gram of tissue. In these experiments the counting efficiency for blood samples was low and was therefore subject to greater measurement error.

The area under the tissue concentration-time curve (AUC) for [^{3}H]TXL was calculated from mean tissue concentration values observed from the time of [^{3}H]TXL or PG-[^{3}H]TXL administration to 144 h after administration (WinNonlin Professional; Scientific Consulting, Lexington, Ky.).

HPLC assay of free TXL release from PG-[^{3}H]TXL

When mice injected with PG-[^{3}H]TXL were killed, a portion of each tissue sample (0.1–0.3 g) was immediately frozen at −70 °C. For analysis of free TXL by HPLC, each frozen tissue sample was thawed and then homogenized with three volumes of PBS (w/v). Up to 200 μl of tissue homogenate was extracted with three volumes of ethyl acetate according to the method of Longnecker et al. [13]. The samples were centrifuged for 5 min at 2500 rpm, and the supernatant was separated and dried. The dried extract was reconstituted with 195 μl HPLC mobile phase and mixed with 5 μl cold TXL (0.2 mg/ml). A total of 100 μl of the reconstituted solution was injected into the HPLC system for the determination of radioactivity from free TXL. The HPLC system consisted of a 150 × 3.9-mm Nova-Pak column, a UV/Vis detector set at 228 nm (Waters, Milford, Mass.), and a flow scintillation analyzer (Packard, Downers Grove, Ill.). The eluting solvent (methanol/water, 2:1) was run at 1.0 ml/min. The

radioactivity due to free TXL is expressed as disintegrations per minute (dpm) per gram of tissue.

Analysis of stability of PG-[^{3}H]TXL in mouse plasma

PG-[^{3}H]TXL in PBS containing 20% C3Hf/kam mouse plasma (2.5 mg/ml) was incubated at 37 °C. At various time intervals, 2-μl aliquots of this solution were removed and applied onto a silica gel thin-layer chromatography plate (Whatman, Clifton, N.J.). Cold TXL in methanol was applied to the same spot to monitor the location of [^{3}H]TXL on the plate. After development with chloroform/methanol (4:1, v/v), silica gel spots containing [^{3}H]TXL (R_f 0.80) and intact PG-[^{3}H]TXL (R_f 0.0) were removed from the plate, and mixed with 0.5 ml methanol and scintillation liquid, and the radioactivity counted. The amount of TXL released is expressed as a percentage of the total applied radioactivity.

Determination of drug elimination

To determine the routes of elimination of [^{3}H]TXL, normal female C3Hf/Kam mice were injected with [^{3}H]TXL (five mice) or PG-[^{3}H]TXL (five mice) at an equivalent TXL dose of 20 mg/kg body weight. The mice were placed in metabolic cages, and urine and feces were collected over two periods: 0–24 h and 24–48 h. The collected samples were analyzed for total radioactivity.

Whole-body autoradiography of mice after i.v. injection of PG-[^{3}H]TXL

Two mice with OCa-1 tumors were injected in the tail vein with PG-[^{3}H]TXL at an equivalent TXL dose of 20 mg/kg (10 μCi in 0.2 ml saline). One mouse was killed 1 day after drug injection, and the other was killed 6 days after drug injection. The bodies were mounted in cryostat cellulose (4%) blocks and frozen, and 100 μm coronal sections were made using a cryostat (LKB 2250 cryo-microtome, Ijamsville, Md.). The sliced sections were dried, exposed to tritium-sensitive phosphor screen for 3 weeks, and imaged with a Cyclone storage phosphor system (Packard, Meriden, Ct.). The data are expressed as digital light units per millimeter squared (DLU/mm^2), and as tissue-to-muscle ratios for each tissue. The system has a linear relationship between radioactivity (dpm/mm^2) and DLU/mm^2.

Data analysis

Statistical values were calculated using the unpaired, two-tailed Student's *t*-test, and *P*-values less than 0.05 were considered statistically significant.

Results

Biodistribution of [^{3}H]TXL and PG-[^{3}H]TXL

After i.v. administration of [^{3}H]TXL, peak plasma concentrations of TXL were achieved within 2 h, and TXL was undetectable in plasma at 5 h after dosing. At 2 h, the highest concentrations of TXL were found in the liver and kidney (Table 1). Between 2 and 24 h after drug administration, tissue concentrations of TXL in the liver and kidney dropped 50-fold and 26-fold, respectively, and concentrations of TXL in the spleen, lung, heart, and muscle declined 9- to 11-fold. In contrast, TXL in the tumor declined only 1.6-fold over the same time period. By 24 h after drug injection, the concentration of TXL was higher in the tumor than in any other tissue tested and remained higher in tumor throughout the 144-h study period.

For PG-[^{3}H]TXL, plasma concentrations peaked at 2 h and were still detectable at 5 h after dosing (Table 2). Based on AUC values, total exposure in blood was 101 times greater following PG-[^{3}H]TXL administration than following [^{3}H]TXL administration, and concentrations of [^{3}H]TXL in tumor tissue were fivefold higher following administration with PG-[^{3}H]TXL compared with [^{3}H]TXL administered in Cremophor vehicle (Table 3, Fig. 1). The highest concentrations of PG-[^{3}H]TXL were observed in the liver, kidney and spleen (Table 2). The lowest PG-[^{3}H]TXL tissue concentrations were in the brain and muscle. In all tissues tested, concentrations of [^{3}H]TXL were higher after PG-[^{3}H]TXL administration than after [^{3}H]TXL administration (Table 3). Tumor-to-muscle ratios were 1.7- to 4.0-fold higher following injection of PG-[^{3}H]TXL than following injection of [^{3}H]TXL (Tables 1 and 2).

Release of [^{3}H]TXL from PG-[^{3}H]TXL

The in vitro release of TXL from PG-[^{3}H]TXL in PBS solution containing 20% mouse plasma was examined using thin-layer chromatography. About 9% of total

Table 1 Tissue distribution of [^{3}H]TXL in female C3Hf/Kam mice after i.v. administration of 20 mg/kg of [^{3}H]TXL. Values are means ± SD (n = 3). (*ND* not detectable; concentrations could not be reliably determined because of low counting efficiency and large variation)

Tissue	[^{3}H]TXL concentration (ng/g tissue)				
	2 h	5 h	24 h	48 h	144 h
Blood	1825 ± 280	ND	ND	ND	ND
Brain	267 ± 31	461 ± 251	383 ± 24	167 ± 108	99 ± 33
Fat	1627 ± 104	1434 ± 713	55 ± 8	54 ± 2	31 ± 2
Heart	3054 ± 617	2856 ± 2649	328 ± 58	235 ± 33	177 ± 116
Kidney	7191 ± 343	3673 ± 1708	275 ± 213	262 ± 8	134 ± 52
Liver	44784 ± 9145	26740 ± 12790	883 ± 92	522 ± 30	213 ± 101
Lung	4730 ± 319	4346 ± 4094	415 ± 90	277 ± 10	203 ± 169
Muscle	2529 ± 570	1261 ± 505	274 ± 108	219 ± 43	78 ± 32
Spleen	2789 ± 2197	2429 ± 804	307 ± 110	288 ± 22	199 ± 94
Tumor	3616 ± 372	4307 ± 1041	2204 ± 605	1326 ± 124	584 ± 370
Tumor/muscle	0.081	0.16	2.49	2.54	2.74

Table 2 Tissue distribution of PG-[^{3}H]TXL in female C3Hf/Kam mice after i.v. administration of the drug at an equivalent TXL dose of 20 mg/kg. Values are means ± SD (n = 3). (*ND* not detectable; concentrations could not be reliably determined because of low counting efficiency and large variation)

Tissue	Equivalent [^{3}H]TXL concentration (ng/g tissue)				
	2 h	5 h	24 h	48 h	144 h
Blood	51510 ± 7056	36855 ± 55	ND	ND	ND
Brain	902 ± 950	2027 ± 1593	235 ± 93	148 ± 31	113 ± 29
Fat	3562 ± 2081	2056 ± 7581	976 ± 309	1027 ± 978	508 ± 88
Heart	16686 ± 2330	9904 ± 3584	5949 ± 1158	3147 ± 905	1282 ± 100
Kidney	47441 ± 4211	60312 ± 8639	40490 ± 13283	16250 ± 2634	2153 ± 190
Liver	53919 ± 34729	49264 ± 1718	90386 ± 33601	60541 ± 6408	43446 ± 27497
Lung	31582 ± 6340	24555 ± 1118	10707 ± 380	5657 ± 1677	1627 ± 260
Muscle	2392 ± 728	1579 ± 230	884 ± 112	459 ± 114	251 ± 50
Spleen	56576 ± 3143	47379 ± 16542	83313 ± 14415	40046 ± 10209	14182 ± 411
Tumor	13573 ± 6470	12241 ± 1900	11859 ± 1709	8630 ± 3011	3249 ± 825
Tumor/muscle	5.67	7.75	13.42	18.80	12.94

Table 3 Area under tissue concentration-time curve (AUC) (ng · h/g tissue) following i.v. administration of PG-[^{3}H]TXL and [^{3}H]TXL to female C3Hf/Kam mice

Tissue	AUC (ng · h/g tissue)		PG-TXL/TXL ratio
	PG-TXL	TXL	
Blood	184,057.5	1,825	101
Brain	43,908.5	28,745	1.5
Fat	138,509	25,752	5
Heart	528,918.5	68,699	8
Kidney	2,730,913.5	86,445	31
Liver	8,337,868.5	466,628.5	18
Lung	996,776.5	94,917.5	11
Muscle	81,943	42,968.5	2
Spleen	5,537,334.5	67,124	82
Tumor	1,097,304	211,395	5

radioactivity was due to free TXL after PG-[^{3}H]TXL was incubated at 37 °C for 24 h (Fig. 2).

To assess the release characteristics of TXL in vivo, the concentrations of free TXL in various tissues after administration of PG-[^{3}H]TXL were measured. While the percentage of free TXL in other tissues remained relatively unchanged at the time-points analyzed, the percentage of radioactivity in the tumor due to free TXL increased from 4% to 17% from 5 h to 144 h after injection of PG-[^{3}H]TXL (Table 4).

Route of elimination

The estimated total urinary excretion in a 48-h period was 5.0% for [^{3}H]TXL and 8.7% for PG-[^{3}H]TXL.

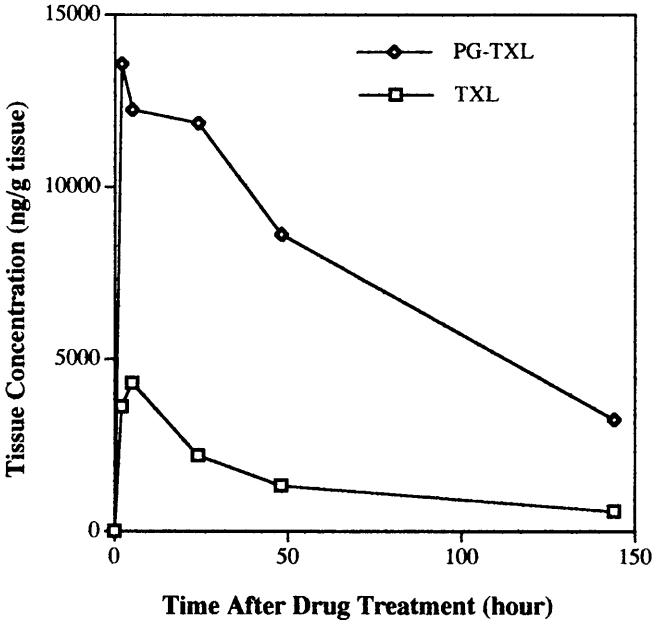

Fig. 1 Concentrations of TXL in the tumor of mice after i.v. administration of PG-[^{3}H]TXL in PBS and [^{3}H]TXL in Cremophor EL/alcohol at an equivalent TXL dose of 20 mg/kg

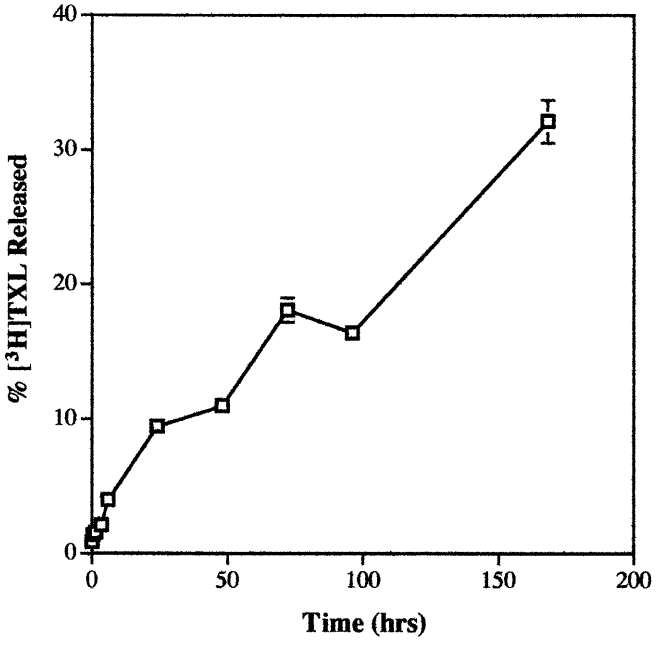

Fig. 2 In vitro release of [^{3}H]TXL from PG-[^{3}H]TXL in PBS solution containing 20% mouse plasma at 37 °C. Aliquots were removed and applied to thin-layer chromatography at various times and the isolated [^{3}H]TXL was quantified using liquid scintillation counting. The values are means ± SD (n = 3)

Table 4 Free TXL tissue concentrations (ng/g tissue) after bolus i.v. injection of PG-[^{3}H]TXL. The radioactivity of [^{3}H]TXL following PG-[^{3}H]TXL injection was determined using an extraction/HPLC procedure (*ND* not detectable)

Tissue	Time after dose (h)		
	5	48	144
Blood	3317 (9%)	ND	ND
Tumor	489 (4%)	949 (11%)	552 (17%)
Liver	2956 (6%)	7265 (12%)	3476 (8%)
Kidney	5428 (9%)	1056 (6.5%)	86 (4%)
Spleen	2369 (5%)	2403 (6%)	993 (7%)

A substantial fraction of the administered dose was recovered in the feces for both drugs. In mice injected with [^{3}H]TXL, approximately 70% of the excreted radioactivity was detected within the first 24 h, whereas in mice injected with PG-[^{3}H]TXL, 30% of the excreted radioactivity was detected in the same time period.

Pattern of drug distribution on radiography

Whole-body autoradiographs of OCa-1 tumor-bearing mice killed 1 and 6 days after i.v. injection of PG-[^{3}H]TXL are shown in Fig. 3. Semiquantitative analysis in selected tissues yielded relative equivalent TXL concentrations. The data expressed as digital light units per millimeter squared (after background correction) and as tissue-to-muscle ratios are displayed in Table 5. The highest concentrations of PG-[^{3}H]TXL 1 day after injection were noted in the liver, kidney, and tumor periphery. Tissue-to-muscle ratios of approximately 20 were found in these areas. When the whole tumor was selected as the region of interest, the tumor-to-muscle ratio was reduced to 13, which was in agreement with the tumor-to-muscle ratio of 13 obtained by the cut-and-count method (Table 2). By day 6, the highest drug concentrations were found in the tumor and liver, and the tissue-to-muscle ratios for these tissues had increased to 56 (Table 5). Qualitative autoradiographic image analysis revealed a homogeneous distribution in the liver parenchyma, the lung, the kidney, and skeletal muscle. However, higher PG-[^{3}H]TXL-derived radioactivity was found in the periphery of the tumor 1 day after injection (Fig. 3A). Activity had diffused into the center of the tumor 6 days after injection, and a more homogenous distribution was revealed (Fig. 3B).

Fig. 3A,B Whole-body autoradiographs of mice killed 1 day (**A**) and 6 days (**B**) after injection of PG-[^{3}H]TXL into the tail vein. The autoradiographs demonstrate high radioactivity in the liver and tumor. The liver has homogeneous distribution of radioactivity, while in the tumor, PG-[^{3}H]TXL-derived radioactivity is significantly higher in the periphery than in the center 1 day after injection (**A**). The PG-[^{3}H]TXL-derived radioactivity 6 days after injection had diffused into the center of tumor (**B**) (*L* liver, *M* muscle; *arrowhead* tumor)

Discussion

Polymer-drug conjugates have been investigated as carriers for anticancer drugs in an attempt to direct active agents to tumors in vivo and to reduce toxic effects on normal tissues [3, 5, 14, 16, 22]. The enhanced antitumor efficacy of polymeric drugs has been shown to be largely attributable to the enhanced permeability and retention (EPR) effect of macromolecules [14]. At present, a few polymer-drug conjugates have reached the stage of clinical application. Conjugation of the rapidly cleared protein drug neocarcinostatin (NCS) to styrene-maleic acid/anhydride copolymer (SMA) greatly improves the drug's stability. The resulting conjugate, SMANCS, has demonstrated significant antitumor activity against hepatocellular carcinoma when administered intraarterially to patients [14]. Hydroxypropyl methacrylamide copolymer (HPMA)-doxorubicin conjugate (PK1) has shown antitumor activity and decreased toxicity relative to doxorubicin in patients with refractory tumors in phase I clinical studies [22]. Both the PK1 and SMANCS conjugates are thought to be internalized by the cell via pinocytosis and then processed intracellularly to release active agents under the action of lysosomal enzymes. Thus, the antitumor efficacy of PK1 varies from tumor to tumor, depending on intratumoral enzyme activity [19].

PG-TXL differs from PK1 and SMANCS in that the linkers between the active drug TXL and the PG carrier polymer are hydrolytically labile ester bonds. Our initial concern was whether premature release of TXL into the

Table 5 Relative TXL concentrations in various tissues determined from autoradiograms of mice injected with 20 mg equivalent TXL/kg PG-[^{3}H]TXL (*DLU* digital light units, *ND* not determined)

Tissue	One day after injection		Six days after injection	
	DLU/mm^2	Tissue/muscle ratio	DLU/mm^2	Tissue/muscle ratio
Muscle	6,586	1.0	784	1.0
Kidney	134,715	20.5	5,953	7.6
Liver	136,014	20.7	43,640	56
Lung	63,592	9.7	2,729	3.5
Whole tumor	66,243	13.0	44,608	57
Tumor periphery	130,570	19.8	ND	ND
Brain	1,580	0.24	186	0.24

plasma and into other normal tissues would undermine its ability to reduce systemic toxicity. As shown in Fig. 2, the fraction of free TXL released in PBS containing mouse plasma during a 48-h period was approximately 10%, which is similar to the fraction of free TXL detected in various tissues examined within a similar time frame after administration of PG-[^{3}H]TXL (Table 4). Since the toxicity of TXL is related to the time that free TXL exceeds a threshold concentration in plasma [21] and plasma concentration of free TXL is relatively low following administration of PG-[^{3}H]TXL due to stability of the inactive PG-TXL conjugate in plasma, toxicity associated with PG-TXL administration is expected to be less than that associated with administration of an equivalent dose of TXL.

The biodistribution of PG-[^{3}H]TXL compared with [^{3}H]TXL administered at an equivalent dose to mice with OCa-1 tumors was consistent with enhanced permeability and retention mechanism for macromolecules. Based on the AUC values calculated from mean tissue concentration data observed from the time of administration to 144 h after administration, tumor exposure to PG-[^{3}H]TXL was fivefold greater than to [^{3}H]TXL following administration of equivalent doses. This is probably attributable to higher plasma concentrations and circulation times of PG-[^{3}H]TXL compared with [^{3}H]TXL. While plasma concentrations of free TXL were low following PG-[^{3}H]TXL administration, the AUC value in blood for PG-[^{3}H]TXL was 101 times greater than following [^{3}H]TXL administration (Table 3). Furthermore, concentrations of free TXL following PG-[^{3}H]TXL administration increased in tumor tissue from 4% to 17% over the 144-h study period (Table 4). These results suggest free TXL may persist in the tumor at higher concentrations for longer time periods following PG-[^{3}H]TXL administration than following [^{3}H]TXL administration. Additional support for enhanced tumor uptake following administration of PG-[^{3}H]TXL was provided by autoradiographic visualization of drug distribution in the tumor. Radioactivity was primarily located in the periphery of the tumor on day 1 after administration of PG-[^{3}H]TXL and had homogeneously diffused into the center of the tumor by day 6 (Fig. 3).

It was noted that the concentrations of PG-[^{3}H]TXL were higher than those of [^{3}H]TXL in all tissues, especially those with more abundant reticular endothelial (RE) systems (i.e. liver, kidney, spleen), suggesting that phagocytosis was involved in the slow elimination of the inactive PG-[^{3}H]TXL macromolecule (Tables 1 and 2). The detection of considerable [^{3}H]TXL-derived radioactivity in the feces and a fast decline in drug concentration in the liver of mice injected with [^{3}H]TXL suggest substantial biliary excretion of TXL. Our data are consistent with the previous finding that hepatic metabolism and biliary excretion is a principal mechanism of TXL elimination [21]. Similarly, the hepatobiliary system is the major site of accumulation and excretion for PG-[^{3}H]TXL. Whether the conjugate is excreted in the form of PG-TXL and/or its degradation products was not determined in the present study.

In summary, this study showed that tumor uptake of PG-TXL was enhanced compared with tumor uptake of TXL injected at the equivalent TXL dose of 20 mg/kg. Furthermore, the amount of free TXL present in tumor tissue persisted for up to 144 h after injection of PG-TXL. Thus, the antitumor activity of PG-TXL observed in preclinical studies may be attributed in part to enhanced tumor uptake of PG-TXL and prolonged release of TXL within the tumor. These results also suggest that the introduction of a hydrolytically labile linker between polymeric carriers and active antitumor agents is a useful approach in the design of macromolecular chemotherapeutic agents.

Acknowledgements We thank Dr. Luka Milas for providing C3Hf/Kam mice. We also thank Nancy Hunter for technical assistance.

References

1. Bartoli M-H, Boitard M, Fessi H, Berrel H, Devissaguet J-P, Picot F, Puisieux F (1990) In vitro and in vivo antitumoral activity of free and encapsulated taxol. J Microencapsul 7: 191–197
2. Beijnen JH, Huizing MT, ten Bokkel Huinink WW, Veenhof CHN, Vermorken JB, Giaccone G, Pinedo HM (1994) Bioanalysis, pharmacokinetics, and pharmacodynamics of the novel anticancer drug paclitaxel (Taxol). Semin Oncol 21 [Suppl 8]: 53–62
3. Berstein A, Hurwitz E, Maron R, Arnon R, Sela M, Wilchek M (1978) Higher antitumor efficacy of daunomycin when linked to dextran: in vitro and in vivo studies. J Natl Cancer Inst 60: 379–384
4. Dorr RT (1994) Pharmacology and toxicology of Cremophor EL diluent. Ann Pharmacother 28: S11–S14

5. Duncan R, Hume IC, Kopeckova P, Ulbrich K, Strohalm J, Kopecek J (1989) Anticancer agents coupled to *N*-(2-hydroxypropyl)methacrylamide copolymers. 3. Evaluation of Adriamycin conjugates against mouse leukemia L1210 in vivo. J Controlled Release 10: 51–63
6. Eiseman JL, Eddington ND, Leslie J, MacAuley C, Sentz DL, Zuhowski M, Kujawa JM, Young D, Egorin M (1994) Plasma pharmacokinetics and tissue distribution of paclitaxel in CD2F1 mice. Cancer Chemother Pharmacol 34: 465–471
7. Goldspiel BR (1994) Paclitaxel pharmaceutical issues: preparation, administration, stability, and compatibility with other medications. Ann Pharmacother 28*:* S23–S26
8. Holmes FA, Kudelka AP, Kavanagh JJ, Huber MH, Ajani JA, Valero V (1995) Current status of clinical trials with Taxol and docetaxel. In: Georg GI, Chen TT, Ojima I, Vyas DM (eds) Taxane anticancer agents: basic science and current status. American Chemical Society, Washington DC, pp 31–57
9. Li C, Yu D-F, Inoue T, Yang DJ, Milas L, Hunter NR, Kim EE, Wallace S (1996) Synthesis and evaluation of water-soluble polyethylene glycol paclitaxel conjugate as a paclitaxel prodrug. Anticancer Drugs 7: 642–648
10. Li C, Yu D-F, Inoue T, Yang DJ, Milas L, Hunter NR, Kim EE, Wallace S (1997) Indium labeled paclitaxel: synthesis, biodistribution and imaging property of ^{111}In-DTPA-paclitaxel in mice bearing mammary tumor. J Nucl Med 38: 1042–1047
11. Li C, Yu D-F, Newman RA, Cabral F, Stephens LC, Milas L, Wallace S (1998) Complete regression of well-established tumors using a novel water-soluble poly(L-glutamic acid)-paclitaxel conjugate. Cancer Res 58: 2404–2409
12. Li C, Price JE, Milas L, Hunter N, Ke S, Yu D-F, Charnsangavej C, Wallace S (1999) Antitumor activity of poly(L-glutamic acid)-paclitaxel on syngeneic and xenografted tumors. Clin Cancer Res 5: 891–897
13. Longnecker SM, Donehower RC, Cates AE, Chen T-L, Brundrett RB, Grochow LB, Ettinger DS, Colvin M (1987) High-performance liquid chromatographic assay for Taxol in human plasma and urine and pharmacokinetics in a phase I trial. Cancer Treat Rep 71: 53–59
14. Maeda H, Seymour LW, Miyamoto Y (1992) Conjugates of anticancer agents and polymers: advantages of macromolecular therapeutics in vivo. Bioconjug Chem 3: 351–362
15. Nicolaou KC, Riemer C, Kerr MA, Rideout D, Wrasidlo W (1993) Design, synthesis and biological activity of protaxols. Nature 364: 464–466
16. Putnam D, Kopecek J (1995) Polymer conjugates with anticancer activity. Adv Polym Sci 122: 55–123
17. Rose WC, Clark JL, Lee FYF, Casazza AM (1997) Preclinical antitumor activity of water-soluble paclitaxel derivatives. Cancer Chemother Pharmacol 39: 486–492
18. Rowinsky EKA, Donehower RC (1995) Paclitaxel (Taxol). N Engl J Med 332: 1004–1014
19. Sat YN, Burger AM, Fiebig HH, Sausville EA, Duncan R (1999) Comparison of vascular permeability and enzymatic activation of the polymeric prodrug HPMA copolymer-doxorubicin (PK1) in human tumor xenografts. Proc Am Assoc Cancer Res 40: 419
20. Sharma A, Straubinger RM (1994) Novel Taxol formulations: preparation and characterization of Taxol-containing liposomes. Pharm Res 11: 889–896
21. Sparreboom A, Tellingen OV, Nooijen WJ, Beijnen JH (1996) Tissue distribution, metabolism and excretion of paclitaxel in mice. Anticancer Drugs 7: 78–86
22. Vasey PA, Kaye SB, Morrison R, Twelves C, Wilson P, Duncan R, Thomson AH, Murray LS, Hilditch TE, Murray T, Burtles S, Fraier D, Frigerio E, Cassidy J (1999) Phase I clinical and pharmacokinetic study of PK1 [*N*-(2-hydroxylpropyl)methacrylamide copolymer doxorubicin]: first member of a new class of chemotherapeutic agents – drug-polymer conjugates. Clin Cancer Res 5: 83–94
23. Weiss RB, Donehower RC, Wiernick PH, Ohnuma T, Gralla RJ, Trump DL, Baker JR, Van Echo DA, Von Hoff DD, Leyland-Jones B (1990) Hypersensitivity reactions from paclitaxel. J Clin Oncol 8: 1263–1268
24. Zhang X, Burt HM, Von Hoff D, Dexter D, Mangold G, Degen D, Oktaba AM, Hunter WL (1997) An investigation of the antitumour activity and biodistribution of polymeric micellar paclitaxel. Cancer Chemother Pharmacol 40: 81–86